BIOCHEMISTRY
including biophysical chemistry & molecular biology

Article

pubs.acs.org/biochemistry

Dominant Intermediate Charcot-Marie-Tooth Disorder Is Not Due to a Catalytic Defect in Tyrosyl-tRNA Synthetase

Clifford A. Froelich[†] and Eric A. First*

Department of Biochemistry and Molecular Biology, Louisiana State University Health Sciences Center in Shreveport, 1501 Kings Highway, Shreveport, Louisiana 71130, United States

ABSTRACT: Charcot-Marie-Tooth disorder (CMT) is the most common inherited peripheral neuropathy, afflicting 1 in every 2500 Americans. One form of this disease, Dominant Intermediate Charcot-Marie-Tooth disorder type C (DI-CMTC), is due to mutation of the gene encoding the cytoplasmic tyrosyl-tRNA synthetase (TyrRS). Three different TyrRS variants have been found to give rise to DI-CMTC: replacing glycine at position 41 by arginine (G41R), replacing glutamic acid at position 196 by lysine (E196K), and deleting amino acids 153−156 (Δ(153−156)). To test the hypothesis that DI-CMTC is due to a defect in the ability of tyrosyl-tRNA synthetase to catalyze the aminoacylation of $tRNA^{Tyr}$, we have expressed each of these variants as recombinant proteins and used single turnover kinetics to characterize their abilities to catalyze the activation of tyrosine and its subsequent transfer to the 3′ end of $tRNA^{Tyr}$. Two of the variants, G41R and Δ(153−156), display a substantial decrease in their ability to bind tyrosine (>100-fold). In contrast, the E196K substitution does not significantly affect the kinetics for formation of the tyrosyl-adenylate intermediate and actually increases the rate at which the tyrosyl moiety is transferred to $tRNA^{Tyr}$. The observation that the E196K substitution does not decrease the rate of catalysis indicates that DI-CMTC is not due to a catalytic defect in tyrosyl-tRNA synthetase.

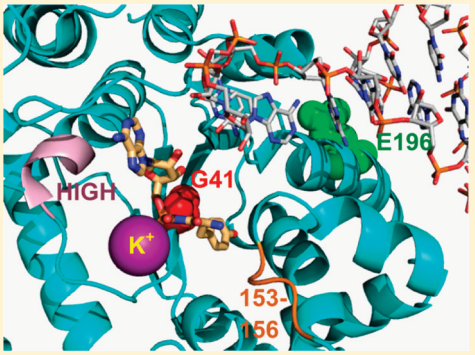

Charcot-Marie-Tooth disorder (CMT) is the most common inherited peripheral neuropathy, afflicting 1 in 2500 people in the United States.[1] CMT affects all ethnic groups, with the onset of symptoms typically occurring in the mid-teens to early adulthood and becoming progressively worse as the patient ages. In CMT, there is a defect in the peripheral nervous system that leads to its degeneration and the subsequent loss of stimulation to the muscles in the hands, feet, arms, and legs. This results in the atrophy and loss of the ability to use these muscles. Charcot-Marie-Tooth disorder may be due to mutations that affect either the Schwann cells that are responsible for the myelin sheath surrounding the peripheral axons or the axons themselves. Damage to the myelin sheath decreases the rate at which the nerve impulses are conducted, while damage to the axon decreases the strength, but not the speed, of the signal.[1−3] There is currently no cure for Charcot-Marie-Tooth disorder.

Mutations in over 30 different genes have been identified as being responsible for various forms of CMT.[4] Four forms of this disorder have been found to be caused by mutations in genes encoding aminoacyl-tRNA synthetases (aaRS), which catalyze the covalent attachment of amino acids to their cognate tRNAs.[5−8] Specifically, mutations in the genes encoding the glycyl- and alanyl-tRNA synthetases give rise to CMT types 2D and 2N, and mutations in the genes encoding the lysyl- and tyrosyl-tRNA synthetases give rise to Recessive Intermediate CMT Type B and Dominant Intermediate CMT Type C (DI-CMTC), respectively.[5−8] In the case of tyrosyl-tRNA synthetase, three different mutations have been shown to give rise to DI-CMTC: substitution of glycine at position 41 by an arginine (G41R), deletion of residues 153−156 (Δ(153−156)), and substitution of a glutamic acid at position 196 by a lysine (E196K).[6] With the exception of Recessive Intermediate CMT Type B, all of the forms of CMT associated with aminoacyl-tRNA synthetases have a dominant inheritance pattern.

As a member of the class I aminoacyl-tRNA synthetase family, tyrosyl-tRNA synthetase plays a central role in protein synthesis. Its primary function is to catalyze the attachment of tyrosine to the 3′ end of $tRNA^{Tyr}$. Aminoacylation of $tRNA^{Tyr}$ occurs in two steps (Figure 1). In the first step, tyrosine is activated by ATP, forming the enzyme-bound tyrosyl-adenylate intermediate (TyrRS·Tyr-AMP). In the second step, tyrosine is transferred to the 3′ end of $tRNA^{Tyr}$ and the tyrosyl-$tRNA^{Tyr}$ and AMP products are released, regenerating the free enzyme. The two steps of the reaction can be run independently of each other, with formation of the tyrosyl-adenylate intermediate being accompanied by a change in the intrinsic fluorescence of the enzyme.[9−11] This allows stopped-flow fluorescence methods to be used to monitor the single-turnover kinetics for each step in the tRNA aminoacylation reaction.[10]

Like other class I aminoacyl-tRNA synthetases, tyrosyl-tRNA synthetase has a Rossmann fold domain that contains the active site and two class I-specific signature sequences, HIGH and KMSKS. While most class I aminoacyl-tRNA synthetases are

Received: June 27, 2011
Revised: July 5, 2011
Published: July 6, 2011

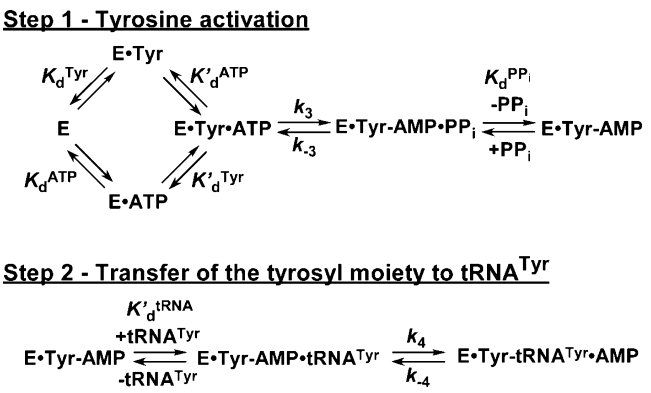

Figure 1. Reaction mechanism for catalysis of tRNA^{Tyr} aminoacylation by tyrosyl-tRNA synthetase. Each step along the reaction pathway for the aminoacylation of tRNA^{Tyr} is shown. Tyrosyl-tRNA synthetase is represented by "E", and "·" and "—" represent noncovalent and covalent bonds, respectively. Dissociation (K_d) and rate (k) constants are shown above and below the step to which they correspond.

functional monomers, tyrosyl-tRNA synthetase (along with the structurally related tryptophanyl-tRNA synthetase) is a homodimer. The observation that tyrosyl-tRNA synthetase displays an extreme form of negative cooperativity, known as "half-of-the-sites reactivity" with respect to tyrosine binding, tyrosyl-adenylate formation, and the binding of tRNA, indicates that the homodimer adopts an asymmetric conformation in solution.[12]

In contrast to bacterial tyrosyl-tRNA synthetases, which have a canonical KMSKS signature sequence, in eukaryotic tyrosyl-tRNA synthetases, the second lysine in the KMSKS sequences is replaced by either a serine or alanine.[13] This is surprising, as this is one of the most highly conserved amino acids in the class I aminoacyl-tRNA synthetase family. The noncanonical KMS-(S/A)S sequence is also present in eukaryotic tryptophanyl-tRNA synthetases and a number of archaeal tyrosyl- and tryptophanyl-tRNA synthetase sequences. In the case of human tyrosyl-tRNA synthetase, an active site potassium ion (K^+) has been shown to functionally replace the second lysine in the KMSKS sequence (i.e., K^+ stabilizes the transition state in human tyrosyl-tRNA synthetase).[14]

The observation that mutations in four different aminoacyl-tRNA synthetase genes give rise to Charcot-Marie-Tooth disorder suggests that a defect in protein synthesis may lead to CMT. The observation that the three mutations associated with DI-CMTC affect amino acids located near either the active site (G41R and Δ(153−156)) or the tRNA binding site (E196K) of tyrosyl-tRNA synthetase further supports this hypothesis (Figure 2). In this paper, we test the hypothesis that the DI-CMTC-associated mutations give rise to a defect in the catalytic activity of tyrosyl-tRNA synthetase. We show that the G41R and Δ(153−156) variants of human tyrosyl-tRNA synthetase are defective in their ability to bind tyrosine and catalyze formation of the enzyme-bound tyrosyl-adenylate intermediate. In contrast, the E196K substitution does not significantly affect the kinetics for formation of the tyrosyl-adenylate intermediate and actually increases the rate at which the tyrosyl moiety is transferred to tRNA^{Tyr}. The observation that the E196K substitution does not decrease the rate of catalysis indicates that DI-CMTC is not due to a catalytic defect in tyrosyl-tRNA synthetase.

A

	G41R	Δ(153-156)	E196K
Homo sapiens	YWGT	VVKQVE	A**E**KYLP
Bos Taurus	YWGT	VVKQVE	A**E**KYLP
Drosophila melanogaster	YWGT	VVKQVE	S**E**KYLP
Caenorhabditis elegans	YWGT	VVKQVE	A**E**EQLP
Saccharomyces cerevisiae	YWGT	VVKQVA	A**E**ENLP
Neurospora crassa	YWGT	VVKQVD	A**K**DWLP
Methanococcus jannaschii	YIGF	I**ARED**E	A**R**ELLP
Bacillus stearotherm.	YCGF	Q**SRIE**T	G**L**ELIR

B

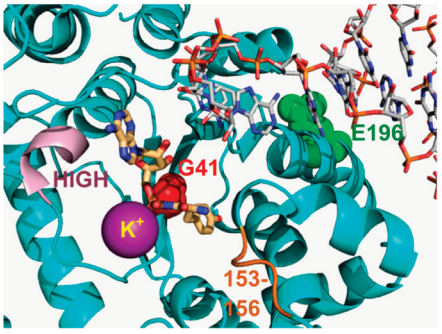

Figure 2. Location of amino acids that are mutated in DI-CMTC. (A) A multiple sequence alignment is shown for the positions of amino acids that are altered in DI-CMTC (altered amino acids are shown in bold). The sequence alignments shown are based on more extensive sequence alignments using ClustalW and include tyrosyl-tRNA synthetase sequences from 11 eukaryotic, 7 archaeal, and 50 bacterial species. (B) The active site structure of human tyrosyl-tRNA synthetase is shown. Tyrosyl-tRNA synthetase is shown in cartoon representation (cyan) with Gly 41, Glu 196, and the active site potassium shown as red, green, and purple space-filled models, respectively. Amino acids 153−156 and the HIGH signature sequence are shown as orange and salmon cartoons, respectively, the nonhydrolyzable tyrosyl-adenylate analogue *O*-(adenosine-5′-*O*-yl) *N*-(L-tyrosyl)-phosphoramidate (TyrAMPN) is shown as thick sticks (CPK color scheme with beige carbon atoms), and the 3′ end of tRNA^{Tyr} is shown as thin sticks (CPK color scheme with gray carbon atoms). The human tyrosyl-tRNA synthetase coordinates are taken from the human TyrRS·tyrosinol structure (PDB 1Q11).[48] The coordinates for the TyrAMPN and tRNA^{Tyr} ligands are taken from the *Saccharomyces cerevisiae* TyrRS·TyrAMPN·tRNA^{Tyr} structure (PDB 2DLC) which has been superimposed onto the Rossmann fold domain of the human TyrRS·tyrosinol structure using the superpose command in the CCP4 software suite.[49−53] After superposition, the tyrosinol in the human TyrRS·tyrosinol structure aligns well with the tyrosyl moiety in the *S. cerevisiae* TyrRS·TyrAMPN·tRNA^{Tyr} structure (average rmsd = 0.72 Å). The 3′-CCA end of tRNA^{Tyr} does not enter the active site in the *S. cerevisiae* TyrRS·TyrAMPN·tRNA^{Tyr} structure, and no attempt has been made to model it into the active site in this figure. Molecular graphics were generated using PyMOL v1.3.[54]

dx.doi.org/10.1021/bi200989h | *Biochemistry* 2011, 50, 7132−7145

EXPERIMENTAL PROCEDURES

Materials. Reagents were purchased from the following sources: [^{14}C]L-tyrosine (Moravek Biochemicals); β-mercaptoethanol (Sigma-Aldrich), inorganic pyrophosphatase (New England Biolabs), Quikchange XL site-directed mutagenesis kit (Stratagene), BA 85 nitrocellulose filters (25 mm) and DE-52 resin (Whatman), Source 15Q-Sepharose anion exchange resin and NAP-25 columns (GE Healthcare), DispoEquilibrium biodialyzer (The Nest Group, Inc.), and EnzChek pyrophosphate assay kit (Invitrogen). All other reagents were purchased from Fisher Scientific and VWR. GraFit version 5.0.6 (Erithacus Software Ltd.) and Kaleidograph version 3.6 (Synergy Software) were used to fit the kinetic data.

Mutation and Purification of the Recombinant Human Tyrosyl-tRNA Synthetase. Construction of the pHYTS3-WT expression plasmid has been previously described.[9,13] pHYTS3-WT consists of the wild-type human cytoplasmic tyrosyl-tRNA synthetase coding sequence subcloned into the pET30a(+) expression plasmid such that the tyrosyl-tRNA synthetase coding sequence immediately follows the enterokinase site in the pET30a(+) vector. Recombinant expression from this construct results in the human tyrosyl-tRNA synthetase containing an amino-terminal His-tag/S-tag fusion that can be removed by enterokinase cleavage. The three mutations known to give rise to DI-CMTC (G41R, Δ(153−156), and E196K) and a Gly 41 to alanine mutation (G41A) were introduced into the human tyrosyl-tRNA synthetase coding sequence in pHYTS3-WT by site-directed mutagenesis using the QuikChange XL site-directed mutagenesis kit and named pHYTS3-G41R, pHYTS3-G41A, pHYTS3-Δ(153−156), and pHYTS3-E196K.

The human tyrosyl-tRNA synthetase variants were expressed in *Escherichia coli* BL21 (DE3) pLysS cells harboring the pHYTS3-WT, pHYTS3-G41R, pHYTS3-G41A, pHYTS3-Δ(153−156), and pHYTS3-E196K vectors. Purification of the recombinant proteins was carried out by nickel affinity chromatography, followed by anion exchange chromatography to remove minor contaminants as previously described.[9,13] SDS-PAGE was used to assess the purity of the human tyrosyl-tRNA synthetase variants.[15] The concentration of the enzyme was determined using a filter-based active-site titration assay as described in ref 12 and from A_{280} measurements in the presence of 6 M guanidine hydrochloride (ε = 89 040 M^{-1} cm^{-1} as determined by the ExPASy ProtParam tool[16]). Purified tyrosyl-tRNA synthetase variants were stored at −70 °C in buffer containing 50 mM Tris, pH 7.5, 20 mM β-mercaptoethanol, 150 mM KCl, 10 mM $MgCl_2$, and 10% glycerol (v/v).

***In Vitro* Transcription and Purification of tRNA^{Tyr}.** The human and *B. stearothermophilus* tRNA^{Tyr} substrates were obtained by *in vitro* transcription from a FokI-linearized pHYR1-WT plasmid as previously described.[17] In contrast to the *B. stearothermophilus* tRNA^{Tyr}, which contains a guanine at the first position, human tRNA^{Tyr} has a cytosine at position 1. As wild-type T7 RNA polymerase requires a guanine at the first position for efficient transcription, the cytosine at position 1 in human tRNA^{Tyr} presents a problem. This was overcome by using a T7 RNA polymerase P266L variant—which is relatively nonspecific with respect to the nucleotide at the first position—to transcribe human tRNA^{Tyr}.[18] *In vitro* transcribed tRNAs were purified by a modification of the procedure described by Sherlin et al.[19] This consists of loading the *in vitro* transcription reaction onto a 5 mL DE52 anion-exchange column equilibrated in buffer A (100 mM HEPES, pH 7.5, 12 mM $MgCl_2$) containing 200 mM NaCl. The tRNA^{Tyr} is eluted from this column using buffer A containing 600 mM NaCl and fractions containing tRNA^{Tyr} (as determined by A_{260} measurements) are pooled and desalted on a NAP-25 size exclusion column. Fractions from the NAP-25 column containing tRNA^{Tyr} are pooled and precipitated by the addition of 7.5 M ammonium acetate (0.5 × volume) and 100% ethanol (2.5 × volume). Following overnight incubation at −20 °C and centrifugation at 12000*g*, the tRNA pellet is dried and resuspended in 500 μL of 10 mM $MgCl_2$. Annealing of tRNA^{Tyr} is achieved by incubation at 80 °C for 10 min, followed by slow cooling at room temperature overnight. The concentration of the *in vitro* transcribed human tRNA^{Tyr} was determined from A_{260} measurements (ε = 742 800 M^{-1} cm^{-1} using the nearest-neighbor method), and plateau levels for aminoacylation of tRNA^{Tyr} were determined using a nitrocellulose filter assay, in which the incorporation of [^{14}C]L-tyrosine into the Tyr-tRNA^{Tyr} product is monitored.[20,21] Comparison of the tRNA concentration and tRNA aminoacylation levels indicates that >90% of the *in vitro* transcribed human tRNA^{Tyr} could be aminoacylated.

Limited Proteolysis. Limited proteolysis was used to study the global stability of the tyrosyl-tRNA synthetase variants using the method described by Park and Marqusee.[22] 12.5 μL of the tyrosyl-tRNA synthetase variant (0.5 mg/mL) was incubated in a 600 μL reaction mixture composed of 0.1 mM $CaCl_2$ and 150 mM KCl. 100 μL aliquots were removed from this reaction mixture, varying concentrations of thermolysin were added such that its final concentration ranged from 0.18 to 13.6 units/μL, and each reaction was incubated for 1 min. The proteolysis reactions were quenched by the addition of 5 μL of EDTA (50 mM, pH 8.0), 20 μL of 6X SDS-PAGE loading buffer (0.35 M Tris, pH 6.8, 30% glycerol 10% SDS, 0.6 M DTT, and 0.012% bromophenol blue) was added to the reaction, and 10 μL aliquots were loaded onto a 12% SDS-PAGE gel for analysis. All reactions were performed at 25 °C. To confirm that the stability of the E196K variant does not significantly differ from that of the wild-type enzyme, 12.5 μL of the wild-type and E196K variants (0.5 mg/mL) were incubated overnight in a 600 μL reaction mixture composed of 0.1 mM $CaCl_2$, 150 mM KCl, and varying concentrations of urea (0−1 M) at 25 °C. After overnight incubation, proteolysis was initiated by the addition of 2 μL of thermolysin (final concentration = 0.4 units/μL). This reaction was allowed to proceed for 1 min following brief vortexing before the reaction was quenched with EDTA. The reactions were analyzed on a 12% SDS-PAGE gel as described above.

Active Site Titration. A modification of the active site titration assay described in ref 23 was used to determine whether any of the tyrosyl-tRNA synthetase variants have a significant defect in their ability to activate tyrosine. In this assay, tyrosyl-tRNA synthetase is incubated with [^{14}C]L-tyrosine (10 μM, 5 μCi/mL), MgATP (2 mM), $MgCl_2$ (10 mM), KCl (150 mM), β-mercaptoethanol (10 mM), inorganic pyrophosphatase (0.01 units/μL), and Tris (144 mM), pH 7.78, at 25 °C. 25 μL aliquots are removed at 2, 5, 10, 20, and 30 min, and the reaction mixture is then passed through a nitrocellulose filter, the filter is washed with cold buffer B (144 mM Tris, 10 mM $MgCl_2$, 150 mM KCl, 10 mM

β-mercaptoethanol, pH 7.78), and the amount of TyrRS·[^{14}C]L-Tyr-AMP bound to the filter is determined by scintillation counting. To determine the percentage of enzyme that has tyrosyl-adenylate bound to it, the concentration of the TyrRS·[^{14}C]L-Tyr-AMP intermediate was divided by the total concentration of enzyme as determined by A_{280} measurements. The data were fit to a first-order rate equation:

$$[\text{TyrRS·Tyr–AMP}]_t = [\text{TyrRS·Tyr–AMP}]_\infty \times (1 - e^{-kt}) \quad (1)$$

where $[\text{TyrRS·Tyr-AMP}]_t$ and $[\text{TyrRS·Tyr-AMP}]_\infty$ are the concentrations of the TyrRS·Tyr-AMP complex at time t and after the reaction is complete, respectively, and k is the rate constant for formation of the TyrRS·Tyr-AMP complex.

Equilibrium Binding Studies. Equilibrium dialysis was performed using DispoEquilibrium biodialyzers as previously described.[12,24] One chamber (chamber A) of each biodialyzer contained 40 μM tyrosyl-tRNA synthetase and 1 unit/mL inorganic pyrophosphatase in buffer B. The other chamber (chamber B) contained concentrations of [^{14}C]L-tyrosine ranging from 40 to 1300 μM in the same buffer. A dialysis membrane with a molecular mass cutoff of 10 000 Da separated the chambers. The biodialyzers were rotated overnight at room temperature to allow the contents in chambers A and B to equilibrate. Following equilibration, the amount of [^{14}C]L-tyrosine present in each chamber was determined by removing 40 μL aliquots, adding each aliquot to 5 mL of Cytoscint scintillation cocktail, and counting the radioactivity using a Beckman LS 6500 scintillation counter. The concentration of tyrosine in each chamber was calculated from the specific activity of the stock [^{14}C]L-tyrosine (100 μCi/mL). The concentrations of enzyme-bound and free tyrosine were calculated by subtracting the tyrosine concentration in chamber B ($[\text{Tyr}]_{\text{free}}$) from that in chamber A ($[\text{Tyr}]_{\text{bound}} + [\text{Tyr}]_{\text{free}}$). The data were then fit to the following equations:[25−27]

$$\alpha = n[\text{Tyr}]_{\text{free}}/(K_d^{\text{Tyr}} + [\text{Tyr}]_{\text{free}}) \quad (2)$$

$$[\text{Tyr}]_{\text{bound}}/[\text{Tyr}]_{\text{free}} = (-1/K_d^{\text{Tyr}})[\text{Tyr}]_{\text{free}} + n[\text{E}]_T/K_d^{\text{Tyr}} \quad (3)$$

where $\alpha = [\text{Tyr}]_{\text{bound}}/[\text{E}]_T$, K_d^{Tyr} is the dissociation constant for tyrosine, n is the total number of binding sites, and $[\text{E}]_T$ is the total enzyme concentration.

Kinetic Procedures. All kinetic analyses were performed in buffer B (144 mM Tris, pH 7.78, 10 mM β-mercaptoethanol, 150 mM KCl, and 10 mM $MgCl_2$) at 25 °C unless otherwise indicated. ATP was added as the Mg^{2+} salt to maintain the free concentration of Mg^{2+} at 10 mM, and the pH was adjusted to 7.8. All kinetic analyses were performed a minimum of three times using tyrosyl-tRNA synthetase from at least two different enzyme preparations.

Tyrosine Activation by the E196K Variant. The kinetics for the activation of tyrosine were analyzed according to Figure 1. In these studies, an SX 18 MV stopped-flow reaction analyzer (Applied Photophysics) is used to monitor the decrease in the intrinsic fluorescence of human tyrosyl-tRNA synthetase on formation of the enzyme-bound tyrosyl-adenylate intermediate (λ_{ex} = 295 nm, λ_{em} > 320 nm).[9,21] The equilibrium constants for the dissociation of ATP from both the TyrRS·ATP and TyrRS·Tyr·ATP complexes (K_d^{ATP} and $K'_d{}^{\text{ATP}}$, respectively) are determined by monitoring formation of the TyrRS·Tyr-AMP intermediate under conditions where the enzyme is initially present as either the unliganded enzyme (i.e., $[\text{Tyr}] \leq 0.1K_d^{\text{Tyr}}$, where K_d^{Tyr} = 34 μM) or as the TyrRS·Tyr complex (i.e., $[\text{Tyr}] \geq 10K_d^{\text{Tyr}}$). Similarly, the equilibrium constant for the dissociation of tyrosine from the TyrRS·Tyr complex (K_d^{Tyr}) is determined by monitoring formation of the TyrRS·Tyr-AMP intermediate under conditions where the enzyme is initially present as the unliganded enzyme (i.e., $[\text{ATP}] \leq 0.1K_d^{\text{ATP}}$, where K_d^{ATP} = 4.7 mM). As concentrations of ATP over 10 mM are inhibitory,[9] the equilibrium constant for the dissociation of tyrosine from the TyrRS·Tyr·ATP complexes ($K'_d{}^{\text{Tyr}}$) is determined by monitoring formation of the TyrRS·Tyr-AMP intermediate in the presence of 10 mM MgATP. Under these conditions, ~70% of the enzyme is present as the TyrRS·ATP complex. The forward rate constant (k_3) is determined from the kinetic experiments used to determine $K'_d{}^{\text{ATP}}$ (i.e., by monitoring formation of the TyrRS·Tyr-AMP intermediate at saturating concentrations of tyrosine).

To determine the equilibrium constant for the dissociation of ATP from the TyrRS·Tyr·ATP complex ($K'_d{}^{\text{ATP}}$), one syringe in the stopped-flow reaction analyzer contained tyrosyl-tRNA synthetase (0.5 μM), inorganic pyrophosphatase (1 unit/mL), and tyrosine (1 M) in buffer B, and the other syringe contained varying amounts of MgATP (0.6−20 mM), inorganic pyrophosphatase (1 unit/mL), and tyrosine (1 M) in buffer B. Equal volumes from each syringe were mixed, and the decrease in the intrinsic fluorescence of the protein was monitored. A minimum of six fluorescence traces were collected and averaged. The resulting average trace was then fit to a single-exponential equation with a floating end point. The equilibrium constant for the dissociation of ATP from the TyrRS·Tyr·ATP complex ($K'_d{}^{\text{ATP}}$) and the forward rate constant for the tyrosine activation reaction (k_3) are calculated from a plot of k_{obs} versus ATP concentration.

Determination of the equilibrium constant for dissociation of ATP from the TyrRS·ATP complex is analogous to the method used to determine $K'_d{}^{\text{ATP}}$, except that the tyrosine concentration is 3 μM. Similarly, determination of the equilibrium constant for the dissociation of tyrosine from the TyrRS·Tyr and TyrRS·Tyr·ATP complexes is analogous to the method used to determine $K'_d{}^{\text{ATP}}$, except that the concentration of ATP is held fixed at 0.3 and 10 mM, respectively, and the concentration of tyrosine is varied from 5 to 200 μM and 5 to 150 μM, respectively.

Pyrophosphorolysis and Pyrophosphate Release. The single turnover kinetics for pyrophosphorolysis of the ATP moiety were monitored by following the increase in the intrinsic fluorescence of the enzyme that occurs on conversion of TyrRS·Tyr-AMP + PP_i to TyrRS·Tyr·ATP (i.e., the reverse of the tyrosine activation reaction) using stopped-flow fluorescence methods.[9,21] The TyrRS·Tyr-AMP intermediate was prepared by incubating tyrosyl-tRNA synthetase with MgATP (10 mM), tyrosine (0.3 mM for wild-type enzyme, 1.5 mM for the E196K variant), and inorganic pyrophosphatase (1 unit/mL) in buffer B for 30 min at 25 °C. The TyrRS·Tyr-AMP complex was separated from free tyrosine and MgATP by gel filtration on a NAP-25 column.[17] The experimental setup for monitoring the reverse reaction is similar to that described above for the activation of tyrosine, except that syringe 1

contains the TyrRS·Tyr-AMP complex (0.3 μM) in buffer C (144 mM Tris buffer, pH 7.78, 10 mM β-mercaptoethanol, 150 mM KCl, and 2.5 mM $MgCl_2$) and syringe 2 contains buffer C and 0.1−0.8 mM disodium pyrophosphate. The concentration of $MgCl_2$ is reduced from 10 mM (in buffer B) to 2.5 mM in buffer C to minimize formation of the $MgPP_i$ salt, which has low solubility in H_2O.

Single-Turnover Kinetic Measurement of $tRNA^{Tyr}$ Aminoacylation. Single turnover kinetics for the transfer of tyrosine to human $tRNA^{Tyr}$ were determined using stopped-flow fluorescence to monitor the increase in the intrinsic fluorescence of the enzyme that occurs on transfer of the tyrosyl moiety to the 3′ end of $tRNA^{Tyr}$.[10,17] The TyrRS·Tyr-AMP intermediate and *in vitro* transcribed $tRNA^{Tyr}$ were prepared and purified as described above. The experimental setup for monitoring the transfer of tyrosine to $tRNA^{Tyr}$ is similar to that described for the activation of tyrosine, except that syringe 1 contains the TyrRS·Tyr-AMP complex (0.3 μM) in buffer D (200 mM HEPES, 20 mM $MgCl_2$, pH 7.5) and syringe 2 contains various concentrations of *in vitro* transcribed $tRNA^{Tyr}$ (1−20 μM) in buffer D.

Steady-State Kinetic Measurement of $tRNA^{Tyr}$ Aminoacylation. Steady-state kinetics for the aminoacylation of *in vitro* transcribed human $tRNA^{Tyr}$ by tyrosyl-tRNA synthetase were determined using the EnzChek pyrophosphate assay kit. In this assay, the production of pyrophosphate from the tRNA aminoacylation reaction is coupled to the conversion of 2-methyl-6-mercapto-7-methylpurine ribonucleoside (MESG) to ribose 1-phosphate and 2-amino-6-mercapto-7-methylpurine, resulting in an increase in absorbance at 360 nm. For the wild-type enzyme, tyrosyl-tRNA synthetase (0.1 μM) was incubated in the presence of L-tyrosine (300 μM), MgATP (1 mM), $MgCl_2$ (10 mM), KCl (150 mM), β-mercaptoethanol (10 mM), inorganic pyrophosphatase (40 units/mL), human placental RNase inhibitor (35 units/mL), purine nucleoside phosphorylase (1 unit/mL), MESG (0.3 mM), PIPES (100 mM), pH 7.5, and varying concentrations of *in vitro* transcribed human $tRNA^{Tyr}$ (3−50 μM). The assay was incubated at 25 °C in a microtiter plate using 100 μL of assay solution for each tRNA concentration and monitored by following the change in absorbance at 360 nm. A_{360} values were converted to micromoles of pyrophosphate released based on a standard curve using known amounts of inorganic pyrophosphate. Steady-state kinetics for the aminoacylation of human $tRNA^{Tyr}$ by the E196K variant of tyrosyl-tRNA synthetase were determined as described above except the concentrations of both tyrosine and MgATP were 0.5 mM and the concentrations of $tRNA^{Tyr}$ used ranged from 1 to 20 μM. Initial rates for the aminoacylation of tRNA were determined by plotting micromoles of pyrophosphate released versus time and fitting the data to a linear equation. These initial rates then were plotted against their corresponding tRNA concentration, and the resulting data were fit to the Michaelis−Menten equation to determine K_m^{tRNA}:[28]

$$v_0 = k_{cat}[E]_t[S]_0/(K_m^{tRNA} + [S]_0) \quad (4)$$

where v_0 is the initial rate, $[E]_t$ is the enzyme concentration, and $[S]_0$ is the initial concentration of $tRNA^{Tyr}$. Because of the formation of precipitate at saturating ATP concentrations, a subsaturating concentration of ATP (1 mM) was used in the assay mix. As a result, it is not possible to determine k_{cat} values for the wild-type and E196K tyrosyl-tRNA synthetase variants from this assay.

Analysis of Kinetic Data. All single turnover kinetic data were fit to a single-exponential floating end-point equation using the Applied Photophysics stopped-flow software package to determine the observed rate constants (k_{obs}). The GraFit and Kaleidagraph software packages were used to plot k_{obs} versus the substrate concentration and to fit these plots to the following hyperbolic function:

$$k_{obs} = k_3[S]_0/(K_d + [S]_0) \quad (5)$$

where k_3 is the forward rate constant for formation of the TyrRS·Tyr-AMP complex, $[S]_0$ is the initial substrate concentration, and K_d is the dissociation constant for the substrate of interest.[29] The Eadie−Hofstee transformation of eq 5 is used to show goodness of fit:[30−32]

$$k_{obs} = -K_d(k_{obs}/[S]_0) + k_3 \quad (6)$$

where k_{obs}, k_3, $[S]_0$, and K_d are defined above.

The forward rate constant for the transfer of the tyrosyl moiety to $tRNA^{Tyr}$ (k_4) and the equilibrium constant for the dissociation of $tRNA^{Tyr}$ from the TyrRS·Tyr-AMP·$tRNA^{Tyr}$ complex ($K'_d{}^{tRNA}$) are calculated using equations that are identical to eqs 5 and 6, except that K_d is replaced by $K'_d{}^{tRNA}$ and k_3 is replaced by k_4.

Calculation of Standard Free Energies of Binding. Relative standard free energies for each state along the tRNA aminoacylation pathway were calculated from the rate and dissociation constants using eqs 7−13, assuming standard states of 1 M for ATP, tyrosine, pyrophosphate, and $tRNA^{Tyr}$:[33]

$$\Delta G^\circ_{TyrRS\cdot Tyr} = RT \ln K_d^{Tyr} \quad (7)$$

$$G^\circ_{TyrRS\cdot Tyr\cdot ATP} = RT \ln(K_d^{Tyr}K'^{ATP}_d) \quad (8)$$

$$\Delta G^{\circ\ddagger}_{TyrRS\cdot[Tyr-ATP]^\ddagger} = RT \ln(k_BT/h) - RT \ln(k_3/K_d^{Tyr}K'^{ATP}_d) \quad (9)$$

$$\Delta G^\circ_{TyrRS\cdot Tyr-AMP\cdot PP_i} = -RT \ln(k_3/k_{-3}K_d^{Tyr}K'^{ATP}_d) \quad (10)$$

$$\Delta G^\circ_{TyrRS\cdot Tyr-AMP} = -RT \ln(k_3K_d^{PPi}/k_{-3}K_d^{Tyr}K'^{ATP}_d) \quad (11)$$

$$\Delta G^\circ_{TyrRS\cdot Tyr-AMP\cdot tRNA} = -RT \ln(k_3K_d^{PPi}/k_{-3}K_d^{Tyr}K'^{ATP}_dK'^{tRNA}_d) \quad (12)$$

$$\Delta G^{\circ\ddagger}_{TyrRS.[Tyr-tRNA.AMP]^\ddagger} = RT \ln(k_BT/h) - RT \ln(k_3k_4K_d^{PPi}/k_{-3}K_d^{Tyr}K'^{ATP}_dK'^{tRNA}_d) \quad (13)$$

where ΔG° is the standard Gibbs free energy change, R is the gas constant, T is the absolute temperature, k_B is the Boltzmann constant, h is Planck's constant, "·" and "−" represent noncovalent and covalent bonds, respectively, and "‡" denotes

dx.doi.org/10.1021/bi200989h | *Biochemistry* 2011, 50, 7132−7145

the transition state complex. Standard free energies for each complex are calculated relative to the standard free energy of the unliganded enzyme.

RESULTS

G41R, G41A, and Δ(153−156) Tyrosyl-tRNA Synthetase Variants Are Impaired in Their Ability To Activate Tyrosine. The coding sequence for wild-type human tyrosyl-tRNA synthetase has previously been subcloned into the pET30a(+) expression vector.[9,13] The three mutations responsible for DI-CMTC, as well as a Gly 41 to alanine substitution, were introduced into the coding sequence for tyrosyl-tRNA synthetase in this vector, generating the following plasmids: pHYTS3-G41R, pHYTS3-G41A, pHYTS3-Δ(153−156), and pHYTS3-E196K. Expression and purification of the recombinant proteins from these vectors results in the tyrosyl-tRNA synthetase variant fused to an amino-terminal His-tag/S-tag. Previous analysis of the recombinant wild-type tyrosyl-tRNA synthetase indicates that the amino-terminal His-tag/S-tag does not affect the kinetics for the activation of tyrosine.[9] SDS-PAGE analysis reveals a single band for each variant, migrating with an apparent molecular mass of ∼65 500 Da (Figure 3, panel A). This is in good agreement with the predicted molecular mass of 69 773 Da and with previously published results for the wild-type human tyrosyl-tRNA synthetase.[13] Comparing the protein concentration determined by active site titration with A_{280} measurements indicates that the wild-type and E196K variants are quantitatively converted to the TyrRS·Tyr-AMP intermediate in less than 2 min (Figure 3, panel B). In contrast, the G41R, G41A, and Δ(153−156) variants are unable to form the TyrRS·Tyr-AMP intermediate complex in significant quantities during the 30 min time course of the active site titration assay (Figure 3, panel B inset). This indicates that there is a severe defect in the ability of these variants to catalyze the tyrosine activation step and is in good agreement with previously published results for these DI-CMTC variants.[34] The observation that formation of TyrRS·Tyr-AMP reaches a maximum at ∼1% of the total enzyme concentration for the G41R, G41A, and Δ(153−156) tyrosyl-tRNA synthetase variants suggests the tyrosyl-adenylate intermediate does not bind tightly to these variants.

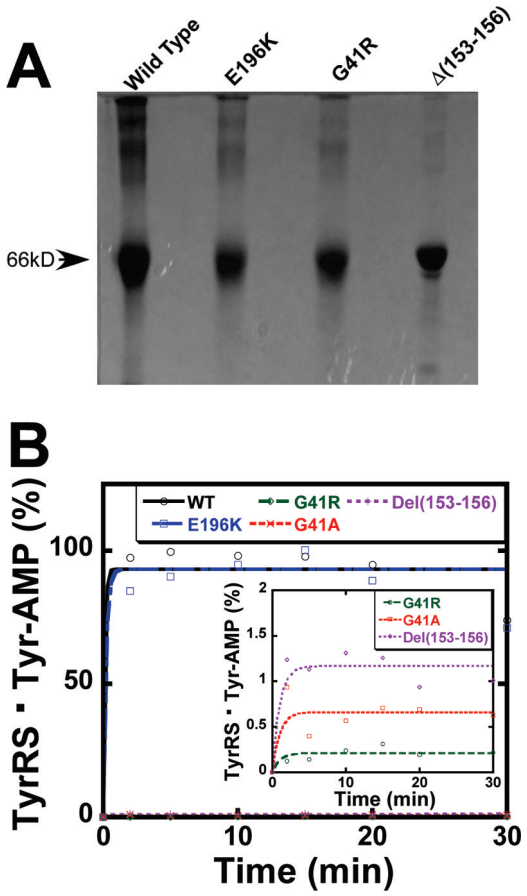

Figure 3. Analysis of purified human tyrosyl-tRNA synthetase variants. (A) SDS-PAGE analysis for purified human tyrosyl-tRNA synthetase variants is shown. (B) A typical plot for formation of the TyrRS·[^{14}C]Tyr-AMP intermediate is shown for the wild-type, G41R, G41A, Δ(153−156), and E196K human tyrosyl-tRNA synthetase variants. Formation of the TyrRS·Tyr-AMP intermediate for the G41R, G41A, and Δ(153−156) variants is replotted on a narrower scale in the inset.

Limited Proteolysis Suggests That Wild-Type Tyrosyl-tRNA Synthetase and the DI-CMTC Variants Have Similar Stabilities. To determine whether the G41R, Δ(153−156), and E196K variants of tyrosyl-tRNA synthetase are less stable than the wild-type enzyme, limited proteolysis experiments were performed using various concentrations of thermolysin. As shown in Figure 4 (panels A−C), no difference is observed between the susceptibility of the wild-type and DI-CMTC variants to proteolysis by thermolysin. While this suggests that the wild-type and variant tyrosyl-tRNA synthetases have similar stabilities, it is possible that the variants are more susceptible to chemical or thermal denaturation. To determine whether this is the case, the wild-type and E196K variants were exposed to varying concentrations of urea (0−1 M) and allowed to equilibrate overnight at 25 °C prior to incubation with 0.006 mg/mL thermolysin. No significant differences are observed in the sensitivity of these proteins to thermolysin (Figure 4, panel D).

Tyrosine Binding Affinity of Tyrosyl-tRNA Synthetase Is Decreased in the G41R, G41A, and Δ(153−156) Variants. Wild-type tyrosyl-tRNA synthetase displays an extreme form of negative cooperativity known as "half-of-the-sites" reactivity with respect to the binding of tyrosine. Equilibrium dialysis was used to determine both the tyrosine dissociation constant for each of the DI-CMTC variants and whether they display half-of-the-sites reactivity. For the G41R, G41A, and Δ(153−156) variants, it is not possible to observe binding by equilibrium dialysis, even when the concentration of tyrosine is 200 μM. As the lower limit for detection of bound tyrosine in this assay is ∼5% of the total enzyme concentration (Figure 5, panel A), the inability to detect tyrosine binding for the G41R, G41A, and Δ(153−156) variants indicates that K_d^{Tyr} is at least 4 mM for these variants.

For the E196K variant, the equilibrium constant for the dissociation of tyrosine from the TyrRS·Tyr complex was determined by both equilibrium dialysis and single turnover kinetics and is similar to that determined for the wild-type enzyme (Figure 5, panels A and B, and Table 1). Equilibrium dialysis indicates that the E196K variant displays half-of-the-sites reactivity with respect to the binding of tyrosine (Figure 5, panel A). Equilibrium dialysis gave a slightly lower value for K_d^{Tyr} than single turnover kinetics (17 μM vs 43 μM, respectively). A similar difference has previously been observed for the wild-type enzyme and has been attributed to differences

dx.doi.org/10.1021/bi200989h | Biochemistry 2011, 50, 7132−7145

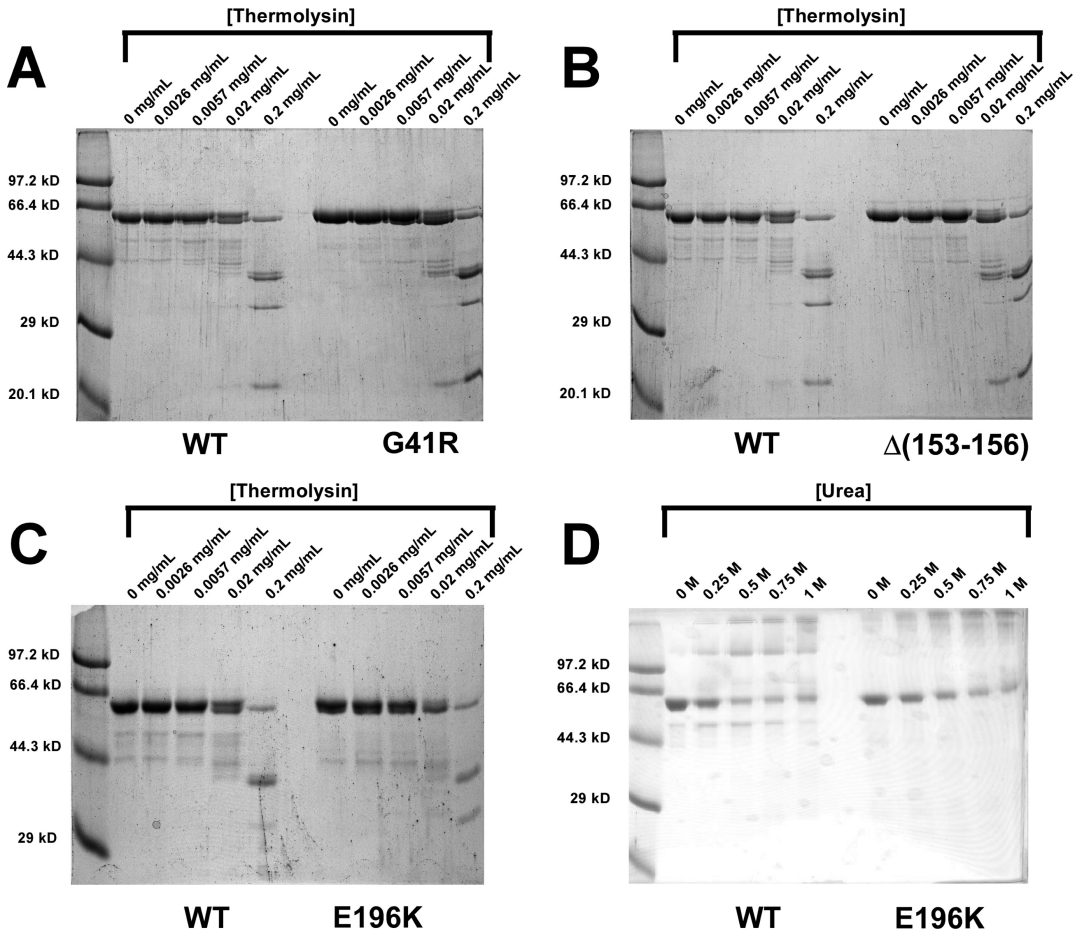

Figure 4. Limited proteolysis of human tyrosyl-tRNA synthetase variants. The results of limited proteolysis experiments for the human tyrosyl-tRNA synthetase variants are shown in the absence (A–C) and presence (D) of urea. Panels A–C contain wild-type tyrosyl-tRNA synthetase and either the G41R, Δ(153–156), or E196K variant, respectively, in the presence of varying concentrations of thermolysin. Panel D contains the wild-type tyrosyl-tRNA synthetase and E196K variant in the presence of varying concentrations of urea and 0.06 mg/mL thermolysin.

in the temperatures at which the equilibrium dialysis and kinetic experiments are performed.[24]

The equilibrium constant for the dissociation of tyrosine from the TyrRS·Tyr·ATP complex was determined using single turnover kinetic methods in the presence of 10 mM MgATP. Under these conditions, the E196K variant displays hyperbolic kinetics and has a tyrosine dissociation constant ($K'_d{}^{Tyr}$) that is identical to that of the wild-type enzyme (Figure 5, panel C, and Table 1).

Wild-Type and E196K Variants Display Similar Affinities for ATP. The equilibrium constants for the dissociation of ATP from the TyrRS·ATP and TyrRS·Tyr·ATP complexes ($K_d{}^{ATP}$ and $K'_d{}^{ATP}$, respectively) were determined using single turnover kinetic methods under conditions where over 90% of the enzyme was present as either the TyrRS·ATP complex (i.e., [Tyr] $\leq 0.1K_d{}^{Tyr}$) or the TyrRS·Tyr·ATP complex (i.e., [Tyr] $\geq 10K_d{}^{Tyr}$). Under these conditions, the E196K variant displays hyperbolic kinetics (Figure 5, panels D and E). The ATP binding affinities for the unliganded TyrRS and TyrRS·Tyr complexes are similar for both the wild-type and E196K variants (Table 1).

The forward rate constant for the tyrosine activation reaction (k_3) was determined by monitoring formation of the TyrRS·Tyr-AMP intermediate at various ATP concentrations in the presence of saturating concentrations of tyrosine (Figure 5, panel E). No difference is observed between the wild-type and E196K variants for the forward rate constant of the tyrosine activation reaction (Table 1).

Wild-Type and E196K Variants Bind Pyrophosphate with Similar Affinities. The kinetics for cleavage of the scissile bond between the α- and β-phosphates of ATP, and the subsequent release of pyrophosphate, were determined by monitoring the conversion of TyrRS·Tyr-AMP + PP_i to TyrRS·Tyr·ATP (i.e., the reverse of the tyrosine activation reaction) using single turnover kinetic methods. The affinity of the E196K variant for pyrophosphate is similar to that of the wild-type enzyme (Figure 5, panel F, and Table 1). The reverse rate constant for the tyrosine activation reaction (k_{-3}) is also similar for the E196K variant and wild-type variants (Table 1).

Kinetic Analysis for Transfer of the Tyrosyl Moiety to $tRNA^{Tyr}$. Until recently, the inability to efficiently synthesize human cytoplasmic $tRNA^{Tyr}$ by *in vitro* transcription has prevented a detailed kinetic analysis of the second step of the $tRNA^{Tyr}$ aminoacylation reaction for human cytoplasmic tyrosyl-tRNA synthetase. This obstacle has been overcome by the discovery of a T7 RNA polymerase P266L variant which has reduced specificity for the nucleotide at the first position of the transcript.[18] *In vitro* transcription reactions catalyzed by this T7 RNA polymerase variant give much higher yields of human

dx.doi.org/10.1021/bi200989h | *Biochemistry* 2011, 50, 7132–7145

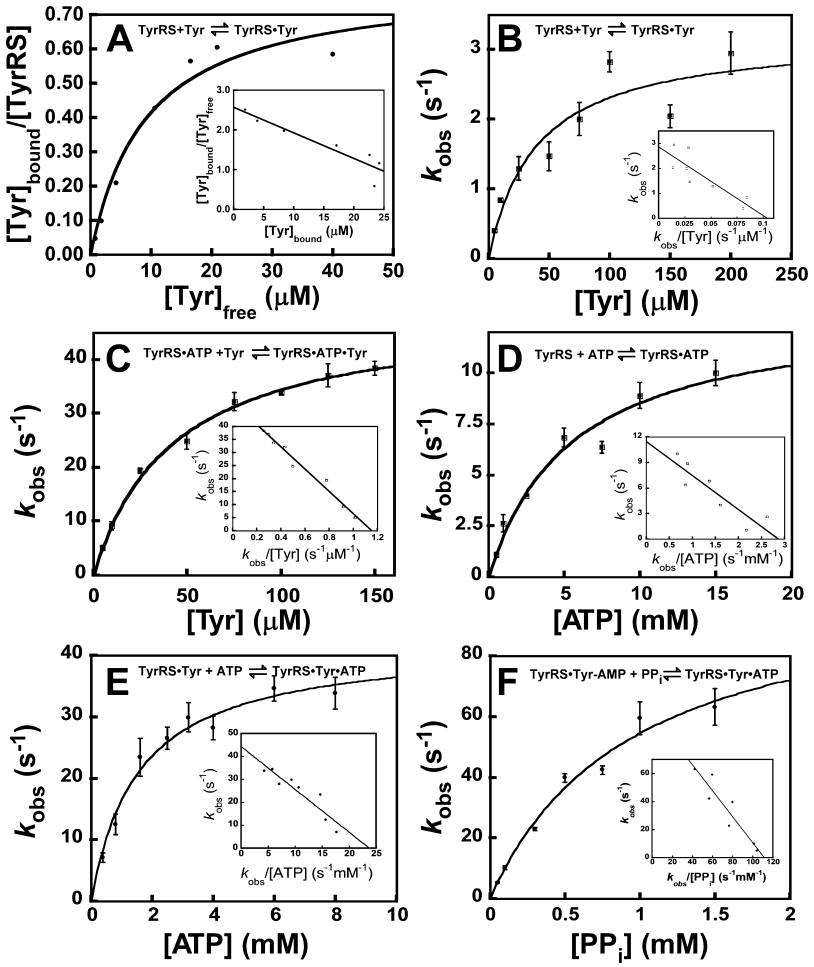

Figure 5. Catalysis of tyrosine activation by the human tyrosyl-tRNA synthetase E196K variant. The equilibrium constant for the dissociation of tyrosine from the TyrRS·Tyr complex (K_d^{Tyr}) was determined by equilibrium dialysis (A) and single turnover kinetics (B) for the E196K variant of human tyrosyl-tRNA synthetase. Equilibrium constants for the dissociation of tyrosine from the TyrRS·Tyr·ATP complex ($K'_d{}^{Tyr}$; panel C), dissociation of ATP from the TyrRS·ATP and TyrRS·Tyr·ATP complexes (K_d^{ATP} and $K'_d{}^{ATP}$; panels D and E, respectively), and dissociation of pyrophosphate from the TyrRS·Tyr-AMP·PP_i complex (K_d^{PPi}; panel F) are also shown. The forward and reverse rate constants (k_3 and k_{-3}) are determined from the single turnover kinetics for dissociation of ATP from the TyrRS·Tyr·ATP complex and dissociation of pyrophosphate from the TyrRS·Tyr-AMP·PP_i complex (panels E and F, respectively). Panel A shows a typical equilibrium dialysis plot. The data are fit to the Langmuir isotherm (eq 2) with a Scatchard plot (eq 3) shown in the inset. Panels B–F are averages of at least three kinetic experiments and are fit to a hyperbolic equation (eq 5) with Eadie–Hofstee transformations (eq 6) shown as insets. The equilibrium reaction that corresponds to the dissociation constant being determined is shown as an inset in each panel. Error bars indicate standard error values.

cytoplasmic $tRNA^{Tyr}$—which contains a C1:G72 base pair—than does the wild-type T7 RNA polymerase. Furthermore, both the yield and aminoacylation kinetics of the *B. stearothermophilus* $tRNA^{Tyr}$ produced by the variant T7 RNA polymerase are similar to those of *B. stearothermophilus* $tRNA^{Tyr}$ produced by wild-type T7 RNA polymerase (data not shown).

Single turnover kinetic methods were used to determine the forward rate constant for transfer of the tyrosyl moiety to $tRNA^{Tyr}$ (k_4) and the equilibrium constant for the dissociation of $tRNA^{Tyr}$ from the TyrRS·Tyr-AMP·$tRNA^{Tyr}$ complex ($K'_d{}^{tRNA}$). As the first step of the reaction (the activation of tyrosine) requires K^+ for full activity,[9,14] the potassium dependence for the second step (transfer of the tyrosyl moiety to the 3′ end of $tRNA^{Tyr}$) was investigated. For the wild-type enzyme, the presence of 150 mM KCl in the assay mix has little effect on either the dissociation constant for $tRNA^{Tyr}$ or the forward rate constant for the second step of the reaction (Figure 6, panels A and C, and Table 1). In the case of the E196K variant, the forward rate constant is ~2-fold greater than that of the wild-type enzyme in the absence of KCl and 13-fold greater than that of the wild-type enzyme in the presence of 150 mM KCl (Figure 6, panels B and D, and Table 1). Surprisingly, deletion of the carboxyl-terminal EMAP II-like domain decreases the forward rate constant for the E196K variant, but not the wild-type enzyme (Table 1). In the absence of KCl, the dissociation constant for $tRNA^{Tyr}$ is similar for the wild-type and E196K variants (Table 1). In the presence of 150 mM KCl, however, the E196K variant has a 3-fold lower affinity for $tRNA^{Tyr}$ than the wild-type enzyme. Deletion of the carboxyl-terminal EMAP II-like domain has no effect on the affinity of the wild-type enzyme for $tRNA^{Tyr}$ but increases the affinity of the E196K variant for $tRNA^{Tyr}$ by 2-fold (Table 1).

Comparison of the above results with previously determined steady-state kinetic analyses of human tyrosyl-tRNA synthetase[35] indicates that the k_4 value obtained from single turnover kinetic analyses is 3-fold lower than the k_{cat} value obtained from

dx.doi.org/10.1021/bi200989h | *Biochemistry* 2011, 50, 7132–7145

Table 1. Single Turnover Kinetic Constants for Wild-Type and E196K Variants of Human Tyrosyl-tRNA Synthetase

TyrRS variant	K_d^{ATP} (mM)	$K'_d{}^{ATP}$ (mM)	k_3 (s^{-1})	K_d^{Tyr} (μM)	$K'_d{}^{Tyr}$ (μM)	k_{-3} (s^{-1})	K_d^{PPi} (mM)	k_4 (s^{-1})	K_d^{tRNA} (μM)
full length wild type						k_{-3}/K_d^{PPi} = 36 s^{-1} M^{-1}[a]			
no KCl	ND[e]	71[a]	1.7[a]	95[a]	ND[c]			0.87 (±0.03)	9.4 (±0.5)
150 mM KCl	4.7 (±0.2)	4[b]	45[b]	34[b]	44[b]	151 (±3)	1.5 (±0.1)	0.56 (±0.06)	4 (±1)
full length E196K									
no KCl	ND[c]	ND[c]	ND[c]	ND[c]	ND[c]	ND[c]	ND[c]	1.45 (±0.04)	12 (±1)
150 mM KCl	6 (±1)	3.0 (±0.7)	42 (±7)	17 (±5)[d]	44 (±4)	110 (±10)	1.0 (±0.2)	8.2 (±0.8)	14 (±1)
mini-TyrRS wild type									
no KCl	ND[c]	ND[c]	ND[c]	ND[c]	ND[c]	ND[c]	ND[c]	0.81 (±0.08)	6.4 (±0.8)
150 mM KCl	ND[c]	ND[c]	ND[c]	ND[c]	ND[c]	ND[c]	ND[c]	0.69 (±0.02)	3.8 (±0.1)
mini-TyrRS E196K									
no KCl	ND[c]	ND[c]	ND[c]	ND[c]	ND[c]	ND[c]	ND[c]	0.81 (±0.02)	4.1 (±0.2)
150 mM KCl	ND[c]	ND[c]	ND[c]	ND[c]	ND[c]	ND[c]	ND[c]	2.9 (±0.1)	6.8 (±0.8)
bacterial (*B. st.*)[e]	3.5[f]	4.7[f]	38[f]	12[f]	ND[c]	16.6[f]	0.61[f]	31[g]	0.39[g]

[a]Values taken from ref 14. [b]Values taken from ref 9. [c]Not determined. [d]Single turnover kinetics gives K_d^{Tyr} = 43 (±8) μM. [e]*B. st.* indicates *Bacillus stearothermophilus* (*Geobacillus stearothermophilus*). [f]Values taken from ref 55. [g]Values taken from ref 10.

steady-state kinetics. Similarly, the K_d^{tRNA} value obtained from single turnover kinetic analyses is 5-fold higher than the previously determined K_m^{tRNA}. To determine whether these differences are due to real differences between the single turnover and steady-state values for these numbers or result from experimental differences, we analyzed the steady-state kinetics for the wild-type and E196K variants of human tyrosyl-tRNA synthetase using the EnzChek pyrophosphate assay. In this assay, the release of pyrophosphate from the tRNA aminoacylation reaction is coupled with the conversion of 2-methyl-6-mercapto-7-methylpurine ribonucleoside (MESG) to ribose 1-phosphate and 2-amino-6-mercapto-7-methylpurine, resulting in an increase in absorbance at 360 nm. Unfortunately, due to the formation of precipitate at saturating ATP concentrations, we were unable to determine k_{cat} values for the tRNA aminoacylation reaction. Using lower ATP concentrations (1 mM), however, allowed us to determine K_m^{tRNA} values for the aminoacylation of human $tRNA^{Tyr}$. As shown in Table 2, the K_m^{tRNA} values for both the wild-type and E196K variants of human tyrosyl-tRNA synthetase are similar to their K_d^{tRNA} values. One possible explanation for the ~3-fold difference between the K_m^{tRNA} value in Table 1 and that determined previously is that the maximum $tRNA^{Tyr}$ concentration used in the previous investigation was only half-saturating and was not sufficient to accurately determine the K_m^{tRNA} value.[35]

Analysis of the Standard Free Energy Profile for the Aminoacylation of $tRNA^{Tyr}$ by Tyrosine. The Gibbs standard free energy values ($\Delta G°$) for each bound state in the reaction pathway are calculated relative to the free energy of the unliganded enzyme for the wild-type and E196K variants of human tyrosyl-tRNA synthetase. Comparing the standard free energy profiles for the wild-type human and *B. stearothermophilus* tyrosyl-tRNA synthetases indicates that for both the TyrRS·Tyr-AMP·tRNA and TyrRS·[Tyr-tRNA·AMP]‡ complexes the human enzyme complexes are less stable than their *B. stearothermophilus* counterparts (Figure 7, panel A). Comparing the activation energies ($\Delta G^{o‡}$) for the tyrosine activation and tyrosyl transfer steps indicates that in human tyrosyl-tRNA synthetase the activation energy for the second step is 10 kJ/mol higher than that for the first step (Figure 7, panel A). This is in constrast to the *B. stearothermophilus* enzyme, where identical activation energies are observed for the two steps.[10] Comparing the free energy profiles for human tyrosyl-tRNA synthetase in the absence and presence of K^+ indicates that potassium exerts its effect on catalysis primarily during the tyrosine activation step (Figure 7, panel B). When K^+ is not present, the transition state for tyrosine activation is destabilized, resulting in identical activation energies for the two steps of the tRNA aminoacylation reaction. Lastly, comparing the free energy profile of wild-type human tyrosyl-tRNA synthetase with that of the E196K variant indicates that the wild-type and E196K variants display similar kinetics (Figure 7, panel C). The one notable difference between the WT and E196K variant is in the activation energy for the second step in the reaction, with the E196K variant displaying 6 kJ/mol lower activation energy than does the wild-type enzyme.

DISCUSSION

Is There a Connection between Protein Synthesis and Charcot-Marie-Tooth Disorder? Dominant intermediate Charcot-Marie-Tooth disorder is characterized by an initial

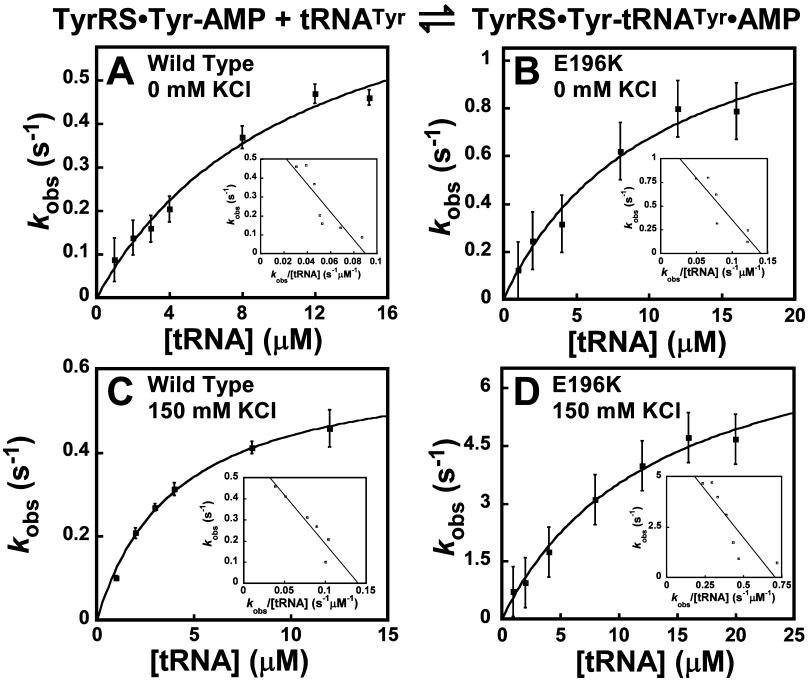

Figure 6. Catalysis of $tRNA^{Tyr}$ aminoacylation by human tyrosyl-tRNA synthetase. The dissociation constant for $tRNA^{Tyr}$ ($K'_d{}^{tRNA}$) and rate constant for tyrosyl transfer (k_4) were determined by single turnover kinetics in the absence and presence of 150 mM KCl for the wild-type (A, C) and E196K (B, D) variants of human tyrosyl-tRNA synthetase. The data are fit to eq 5 with Eadie−Hofstee transformations (eq 6) shown as insets. Error bars indicate standard error values.

Table 2. Comparison of Steady-State Kinetic Constants for Tyrosyl-tRNA Synthetases

organism[a]	$K_m{}^{tRNA}$ (μM)	k_{cat} (s^{-1})	ref
human[b]	4.5 (±0.3)		this paper
human (E196K)[b,c]	10 (±1)		this paper
human[c]	0.9	1.49	35
bovine	0.69	0.05	56
rat	0.14		57
Drosophila melanogaster	0.3		58
baker's yeast	2.0	1.5	45
S. cerevisiae	0.35	6.1	59
wheat germ	3.3		60
B. stearotherm	1.40	4.0	10
E. coli	15	6.3	21

[a]All kinetic constants correspond to the wild-type enzyme with the exception of the E196K variant of human tyrosyl-tRNA synthetase. [b]k_{cat} values could not be determined because the assay was performed at subsaturating ATP concentrations. Standard error values are shown in parentheses. [c]The maximum tRNA concentration used in the assay was $\leq 2K_m$.

weakness in the lower limbs. As the disease progresses, there is severe weakness and atrophy of the distal leg and intrinsic hand muscles.[36,37] Peripheral nerve biopsy indicates these symptoms are due to chronic axonal degeneration with secondary segmental demyelination.[36,37] Jordanova et al. identified three mutations in the gene encoding tyrosyl-tRNA synthetase that are responsible for DI-CMTC.[6] The observation that these three mutations, G41R, Δ(153−156), and E196K, are all located near the active site suggests that DI-CMTC may be due to a catalytic defect in the human cytoplasmic tyrosyl-tRNA synthetase. In this paper, we have used single turnover kinetic methods to test this hypothesis. Although the observation that the G41R substitution and Δ(153−156) deletion decrease the tyrosine binding affinity by more than 2 orders of magnitude is consistent with the above hypothesis, the observation that the E196K variant is actually more active than the wild-type enzyme indicates that DI-CMTC cannot be due to a catalytic defect in the human cytoplasmic tyrosyl-tRNA synthetase. Furthermore, the observation that the stabilities of the G41R, Δ(153−156), and E196K variants are similar to that of the wild-type enzyme suggests that DI-CMTC is not due to destabilization of the enzyme. These results are consistent with the observations that (1) the dominant inheritance pattern of DI-CMTC suggests the mutations should give rise to a gain-of-function phenotype, not a loss of catalytic activity, and (2) tyrosyl-tRNA synthetase haploinsufficiency fails to produce a CMT-like phenotype in a *Drosophila melanogaster* model of DI-CMTC.[34,38]

If DI-CMTC is not due to a defect in catalytic activity, how do mutations in the gene encoding tyrosyl-tRNA synthetase give rise to this disorder? A number of aminoacyl-tRNA synthetases, including tyrosyl-tRNA synthetase, have non-canonical activities that are unrelated to their roles in protein synthesis. For example, during apoptosis human tyrosyl-tRNA synthetase is secreted from the cell and subsequently cleaved, releasing a pro-inflammatory and anti-angiogenic carboxyl-terminal domain and a pro-angiogenic amino-terminal domain.[39] However, the observation that none of the mutations associated with DI-CMTC are located in regions responsible for these noncanonical functions suggests that they do not play a role in DI-CMTC. Furthermore, the four aminoacyl-tRNA synthetases associated with CMT do not appear to share similar noncanonical functions,[40] although it is conceivable that they have noncanonical functions that have not yet been identified. Assuming mutation of these aminoacyl-tRNA synthetases gives rise to CMT via a common mechanism, if noncanonical functions are involved, all four aminoacyl-tRNA synthetases

dx.doi.org/10.1021/bi200989h | *Biochemistry* 2011, 50, 7132−7145

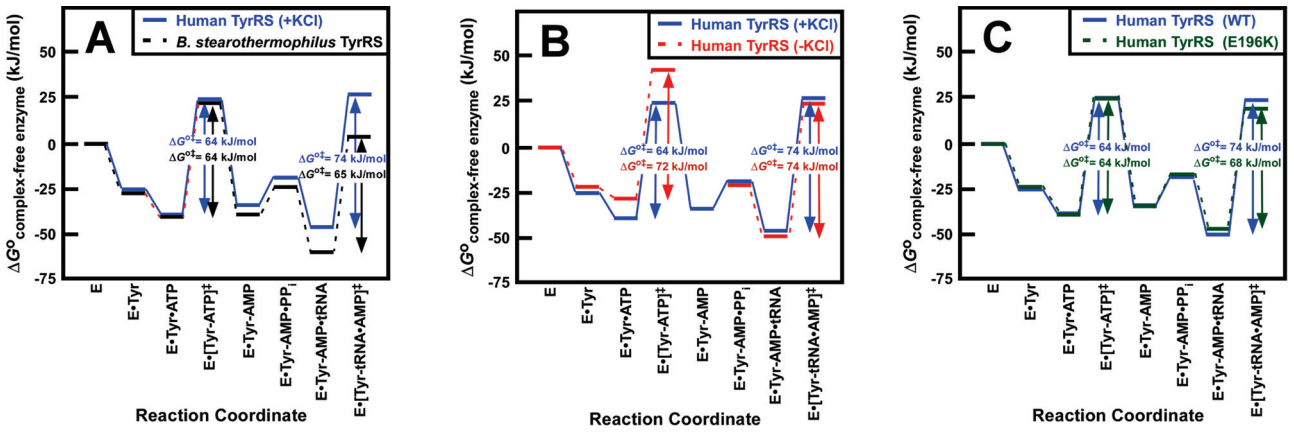

Figure 7. Standard free energy diagrams for the aminoacylation of $tRNA^{Tyr}$. (A) Standard free energy diagrams comparing wild-type human tyrosyl-tRNA synthetase (blue, solid line) to the *B. stearothermophilus* tyrosyl-tRNA synthetase (black, dashed line) are shown. (B) Standard free energy diagrams comparing wild-type human tyrosyl-tRNA synthetase in the presence (blue, solid line) and absence (red, dashed line) of 150 mM KCl are shown. The TyrRS·Tyr-AMP·PP_i complex is not shown for wild-type tyrosyl-tRNA synthetase in the absence of KCl because the reverse rate constant (k_{-3}) and dissociation constant for pyrophosphate (K_d^{PPi}) could not be independently determined. (C) Standard free energy diagrams comparing the wild-type (blue, solid line) and E196K (green, dashed line) variants of human tyrosyl-tRNA synthetase are shown. Standard free energy values for the activation of tyrosine by the wild-type human tyrosyl-tRNA synthetase are taken from ref 9. Standard free energy values for wild type *B. stearothermophilus* tyrosyl-tRNA synthetase are taken from refs 10 and 33. For all panels, activation energies ($\Delta G^{o\ddagger}$) are overlaid onto the transition states to which they correspond.

would need to share the same (currently unknown) non-canonical function.

A second possibility is that the DI-CMTC mutations alter the association of tyrosyl-tRNA synthetase with other proteins in the cell. There is precedent for this proposal, as mutations in Cu, Zn-superoxide dismutase that give rise to an amyotrophic lateral sclerosis phenotype in mice lead to the association of the variant superoxide dismutase with mitochondrial lysyl-tRNA synthetase. This interaction results in misfolding of the mitochondrial lysyl-tRNA synthetase, impairing its importation into the mitochondria.[41] It is possible that mutation of the tyrosyl- (and perhaps glycyl-, alanyl-, and lysyl-) tRNA synthetase(s) results in its association with a protein in the peripheral nerve cells. This could lead to either destabilization or mislocalization of the aminoacyl-tRNA synthetase or the protein to which it is bound, impairing the function of the nerve cell. Transfection of neuroblastoma cells with the G41R and E196K tyrosyl-tRNA synthetase variants results in mislocalization of the variants.[6] Similarly, transfecting neuroblastoma cells with CMT-2D mutants results in mislocalization of the glycyl-tRNA synthetase variants.[42] These observations are consistent with the hypothesis that DI-CMTC and CMT-2D result from inappropriate association of the tyrosyl- and glycyl-tRNA synthetase variants with neuronal proteins.

A third possibility is that it is not a loss of catalytic activity that leads to CMT, but a decrease in the fidelity of the tRNA aminoacylation reaction. In this case, misacylation of tRNA would increase the overall level of protein misfolding in the cell. This hypothesis is intriguing, as it is consistent with the dominant inheritance pattern of DI-CMTC and suggests that the molecular defect is similar to that proposed for other late-onset neurodegenerative diseases, such as Alzheimer's, Huntington's, and Parkinson's diseases.[43] The observation that a mutation in the editing domain of alanyl-tRNA synthetase leads to the loss of cerebellar Purkinje cells and ataxia in mice indicates that decreasing the fidelity of tRNA aminoacylation can affect neuronal cells.[44] Further support comes from preliminary evidence in our laboratory that the human tyrosyl-tRNA synthetase E196K variant has decreased fidelity compared to that of the wild-type enzyme (manuscript in preparation).

Why Is Transfer of the Tyrosyl Moiety to $tRNA^{Tyr}$ Slower for Human Tyrosyl-tRNA Synthetase than It Is for the Bacterial Enzyme? Single turnover kinetic analyses of *B. stearothermophilus* tyrosyl-tRNA synthetase revealed that the two steps in the aminoacylation reaction (tyrosine activation and transfer of the tyrosyl moiety to tRNA) have identical activation energies.[10] Avis and Fersht postulate that there is selective pressure to maintain equal activation energies for the two steps, since stabilizing one transition state will make the other transition state rate-limiting.[10] It is therefore surprising that, in human tyrosyl-tRNA synthetase, the standard free energy of the transition state for transfer of the tyrosyl moiety to $tRNA^{Tyr}$ is 10 kJ/mol higher than it is for the tyrosine activation step of the reaction (Figure 7, panel A). One possible explanation for this observation is that post-translational modification of the human $tRNA^{Tyr}$ substrate is required for optimal catalysis. Several lines of evidence indicate that this is unlikely, however. First, steady-state kinetic analysis of human tyrosyl-tRNA synthetase indicates that the previously published value of k_{cat} is similar to the k_4 value determined by single turnover kinetics (Table 2). Second, comparison of k_{cat} values for other eukaryotic tyrosyl-tRNA synthetases indicates that they are generally lower than the k_{cat} values determined for bacterial tyrosyl-tRNA synthetases (Table 2). Third, direct comparison of the aminoacylation of modified and unmodified $tRNA^{Tyr}$ from *Saccharomyces cerevisiae* indicates that there is at most a 3-fold increase in k_{cat} for the modified $tRNA^{Tyr}$ relative to unmodified $tRNA^{Tyr}$.[45] Lastly, these observations are consistent with kinetic analysis of $tRNA^{Tyr}$ aminoacylation by *B. stearothermophilus* tyrosyl-tRNA synthetase, which indicates that post-transcriptional modification of the $tRNA^{Tyr}$ substrate has little effect on the forward rate constant for tyrosyl transfer, k_4.[10] These observations suggest that it is the transfer of the tyrosyl moiety to the 3′ end of $tRNA^{Tyr}$ that is rate-limiting in eukaryotic tyrosyl-tRNA synthetases. It should be noted that, in

dx.doi.org/10.1021/bi200989h | *Biochemistry* 2011, 50, 7132–7145

contrast to other class I aminoacyl-tRNA synthetases, release of the aminoacyl-tRNA product is not the rate-limiting step for bacterial tyrosyl-tRNA synthetases.[10,46] The observation that the k_4 and k_{cat} values are similar for human tyrosyl-tRNA synthetase suggests that this is also the case for eukaryotic tyrosyl-tRNA synthetases.

The observation that transfer of the tyrosyl moiety to tRNA is rate-limiting in human tyrosyl-tRNA synthetase raises the question as to why there is not selective pressure to maintain equal activation energies for the two steps in the $tRNA^{Tyr}$ aminoacylation reaction. One clue comes from the observation that, in the absence of K^+, the activation energies for the two steps are identical (Figure 7, panel B). This suggests that, prior to the introduction of K^+ into the active site, there was selective pressure to maintain equal activation energies. One implication of this hypothesis is that the appearance of the noncanonical KMSSS signature sequence in eukaryotic tyrosyl-tRNA synthetases preceded the introduction of the potassium ion into the active site. Even if this scenario is correct, however, it does not explain why the rate of catalysis for the second step did not evolve to match the faster catalytic rate for the first step after K^+ became a part of the catalytic mechanism of the enzyme. The observation that the activation energy for the second step is 6 kJ/mol lower in the E196K variant than it is in the wild-type enzyme (Figure 7, panel C) indicates that it is possible to further stabilize the transition state for the tyrosyl transfer step. One possible explanation for the unequal activation energies in the wild-type enzyme is that the lower rate for the aminoacyl transfer step increases the specificity of the enzyme by allowing the aminoacyl-adenylate to remain bound to the enzyme for a longer period of time. This could have two effects. First, it gives non-cognate tRNAs, which bind less tightly than the cognate $tRNA^{Tyr}$, more time to dissociate, thereby increasing the specificity of the enzyme with respect to the tRNA substrate. Second, it increases the probability that enzyme-catalyzed hydrolysis of the aminoacyl-adenylate occurs. If the rate of hydrolysis for noncognate aminoacyl-adenylates is greater than that for tyrosyl-adenylate, then delaying the transfer of the aminoacyl moiety to tRNA could increase the specificity of the enzyme with respect to its amino acid substrate via a pretransfer editing mechanism. A caveat to this mechanism is that it remains to be shown that pretransfer editing occurs in tyrosyl-tRNA synthetase. In this regard, it is interesting to note that enzyme-catalyzed pretransfer editing has been observed for the class II seryl-tRNA synthetase which, like tyrosyl-tRNA synthetase, lacks an editing domain.[47] One prediction of the above hypothesis is that the E196K variant will display a lower fidelity than the wild-type enzyme with respect to either the amino acid or tRNA substrate, leading to the misincorporation of amino acids during protein synthesis.

CONCLUDING REMARKS

Four forms of Charcot-Marie-Tooth disorder are caused by mutations in the genes encoding aminoacyl-tRNA synthetases, suggesting a connection between CMT and protein synthesis. In this paper, we show that DI-CMTC is not due to a catalytic defect in tyrosyl-tRNA synthetase. The hypothesis that a loss of fidelity in tyrosyl-tRNA synthetase gives rise to DI-CMTC is particularly attractive as it provides an explanation for the dominant inheritance pattern and links the molecular basis of this disease to other late-onset neurological disorders. Preliminary evidence in our laboratory supports this hypothesis (manuscript in preparation).

AUTHOR INFORMATION

Corresponding Author

*E-mail: efirst@lsuhsc.edu. Phone: (318) 675-7779. Fax: (318) 675-5180.

Present Address

[†]Department of Structural Biology, MS 311, Room D-1034G, St. Jude Children's Research Hospital, 262 Danny Thomas Place, Memphis, TN 38105-3678.

Funding

This work was supported by Muscular Dystrophy Association grant no. 4268.

ACKNOWLEDGMENTS

We thank Marc Chaudoir, Tara Andrews, Anita Sheoran, Gyanesh Sharma, and Charles Richardson for technical assistance and advice and Dr. Marc Dreyfus for his donation of the T7 RNA polymerase P266L clone.

ABBREVIATIONS

CMT, Charcot-Marie-Tooth disorder; DI-CMTC, Dominant Intermediate Charcot-Marie-Tooth Disorder Type C; CMT-2D; MESG, 2-methyl-6-mercapto-7-methylpurine ribonucleoside; aaRS, aminoacyl-tRNA synthetase; TyrRS, tyrosyl-tRNA synthetase; AA, amino acid; TyrAMP, tyrosyl-adenylate; TyrAMPN, *O*-(adenosine-5′-*O*-yl) *N*-(L-tyrosyl)-phosphoramidate; PP_i, pyrophosphate; EMAP II, endothelial monocyte activating polypeptide II; PDB, Protein Data Bank.

REFERENCES

(1) Charcot-Marie-Tooth Disease Fact Sheet (2003), National Institute of Neurological Disorders and Stroke (NINDS), Washington, D.C.

(2) Bertorini, T., Narayanaswami, P., and Rashed, H. (2004) Charcot-Marie-Tooth disease (hereditary motor sensory neuropathies) and hereditary sensory and autonomic neuropathies. *Neurologist 10*, 327−337.

(3) Shy, M. E. (2006) Peripheral neuropathies caused by mutations in the myelin protein zero. *J. Neurol. Sci. 242*, 55−66.

(4) Timmerman, V. (2007) Inherited Peripheral Neuropathies Database, HUGO Mutation Database Initiative.

(5) Antonellis, A., Ellsworth, R. E., Sambuughin, N., Puls, I., Abel, A., Lee-Lin, S. Q., Jordanova, A., Kremensky, I., Christodoulou, K., Middleton, L. T., Sivakumar, K., Ionasescu, V., Funalot, B., Vance, J. M., Goldfarb, L. G., Fischbeck, K. H., and Green, E. D. (2003) Glycyl tRNA synthetase mutations in Charcot-Marie-Tooth disease type 2D and distal spinal muscular atrophy type V. *Am. J. Hum. Genet. 72*, 1293−1299.

(6) Jordanova, A., Irobi, J., Thomas, F. P., Van Dijck, P., Meerschaert, K., Dewil, M., Dierick, I., Jacobs, A., De Vriendt, E., Guergueltcheva, V., Rao, C. V., Tournev, I., Gondim, F. A., D'Hooghe, M., Van Gerwen, V., Callaerts, P., Van Den Bosch, L., Timmermans, J. P., Robberecht, W., Gettemans, J., Thevelein, J. M., De Jonghe, P., Kremensky, I., and Timmerman, V. (2006) Disrupted function and axonal distribution of mutant tyrosyl-tRNA synthetase in dominant intermediate Charcot-Marie-Tooth neuropathy. *Nature Genet. 38*, 197−202.

(7) Latour, P., Thauvin-Robinet, C., Baudelet-Mery, C., Soichot, P., Cusin, V., Faivre, L., Locatelli, M. C., Mayencon, M., Sarcey, A., Broussolle, E., Camu, W., David, A., and Rousson, R. (2010) A major determinant for binding and aminoacylation of tRNA(Ala) in

cytoplasmic Alanyl-tRNA synthetase is mutated in dominant axonal Charcot-Marie-Tooth disease. *Am. J. Hum. Genet. 86*, 77−82.

(8) McLaughlin, H. M., Sakaguchi, R., Liu, C., Igarashi, T., Pehlivan, D., Chu, K., Iyer, R., Cruz, P., Cherukuri, P. F., Hansen, N. F., Mullikin, J. C., Biesecker, L. G., Wilson, T. E., Ionasescu, V., Nicholson, G., Searby, C., Talbot, K., Vance, J. M., Zuchner, S., Szigeti, K., Lupski, J. R., Hou, Y. M., Green, E. D., and Antonellis, A. (2010) Compound heterozygosity for loss-of-function lysyl-tRNA synthetase mutations in a patient with peripheral neuropathy. *Am. J. Hum. Genet. 87*, 560−566.

(9) Austin, J., and First, E. A. (2002) Catalysis of tyrosyl-adenylate formation by the human tyrosyl-tRNA synthetase. *J. Biol. Chem. 277*, 14812−14820.

(10) Avis, J. M., Day, A. G., Garcia, G. A., and Fersht, A. R. (1993) Reaction of modified and unmodified tRNA(Tyr) substrates with tyrosyl-tRNA synthetase (Bacillus stearothermophilus). *Biochemistry 32*, 5312−5320.

(11) Fersht, A. R., Mulvey, R. S., and Koch, G. L. (1975) Ligand binding and enzymic catalysis coupled through subunits in tyrosyl-tRNA synthetase. *Biochemistry 14*, 13−18.

(12) Fersht, A. R. (1975) Demonstration of two active sites on a monomeric aminoacyl-tRNA synthetase. Possible roles of negative cooperativity and half-of-the-sites reactivity in oligomeric enzymes. *Biochemistry 14*, 5−12.

(13) Kleeman, T. A., Wei, D., Simpson, K. L., and First, E. A. (1997) Human tyrosyl-tRNA synthetase shares amino acid sequence homology with a putative cytokine. *J. Biol. Chem. 272*, 14420−14425.

(14) Austin, J., and First, E. A. (2002) Potassium functionally replaces the second lysine of the KMSKS signature sequence in human tyrosyl-tRNA synthetase. *J. Biol. Chem. 277*, 20243−20248.

(15) Laemmli, U. K. (1970) Cleavage of structural proteins during the assembly of the head of bacteriophage T4. *Nature 227*, 680−685.

(16) Gasteiger, E., Hoogland, C., Gattiker, A., Duvaud, S., Wilkins, M. R., Appel, R. D., and Bairoch, A. (2005) Protein Identification and Analysis Tools on the ExPASy Server, in *The Proteomics Protocols Handbook* (Walker, J. M., Ed.) 1st ed., pp 571−608, Humana Press, New York.

(17) Xin, Y., Li, W., and First, E. A. (2000) The 'KMSKS' motif in tyrosyl-tRNA synthetase participates in the initial binding of tRNA(Tyr). *Biochemistry 39*, 340−347.

(18) Guillerez, J., Lopez, P. J., Proux, F., Launay, H., and Dreyfus, M. (2005) A mutation in T7 RNA polymerase that facilitates promoter clearance. *Proc. Natl. Acad. Sci. U.S.A. 102*, 5958−5963.

(19) Sherlin, L. D., Bullock, T. L., Nissan, T. A., Perona, J. J., Lariviere, F. J., Uhlenbeck, O. C., and Scaringe, S. A. (2001) Chemical and enzymatic synthesis of tRNAs for high-throughput crystallization. *RNA 7*, 1671−1678.

(20) Tataurov, A.V., You, Y., and Owczarzy, R. (2008) Predicting ultraviolet spectrum of single stranded and double stranded deoxyribonucleic acids. *Biophys. Chem. 133*, 66−70.

(21) Jakes, R., and Fersht, A. R. (1975) Tyrosyl-tRNA synthetase from Escherichia coli. Stoichiometry of ligand binding and half-of-the-sites reactivity in aminoacylation. *Biochemistry 14*, 3344−3350.

(22) Park, C., and Marqusee, S. (2006) Quantitative determination of protein stability and ligand binding by pulse proteolysis. *Curr. Protoc. Protein Sci.*, Chapter 20, Unit 20 11.

(23) Fersht, A. R., Ashford, J. S., Bruton, C. J., Jakes, R., Koch, G. L., and Hartley, B. S. (1975) Active site titration and aminoacyl adenylate binding stoichiometry of aminoacyl-tRNA synthetases. *Biochemistry 14*, 1−4.

(24) Sheoran, A., Sharma, G., and First, E. A. (2008) Activation of D-tyrosine by Bacillus stearothermophilus tyrosyl-tRNA synthetase: 1. Pre-steady-state kinetic analysis reveals the mechanistic basis for the recognition of D-tyrosine. *J. Biol. Chem. 283*, 12960−12970.

(25) Clarke, A. R. (1966) Analysis of Ligand Binding by Enzymes, in *Enzymology Labfax* (Engel, P., Ed.) 1st ed., Chapter 6, pp 201−205, Academic Press, New York.

(26) Langmuir, I. (1916) The constitution and fundamental properties of solids and liquids, I - Solids. *J. Am. Chem. Soc. 38*, 2221−2295.

(27) Scatchard, G. (1948) The attactions of proteins for small molecules and ions. *Ann. N.Y. Acad. Sci. 51*, 660−672.

(28) Michaelis, L., and Menten, M. (1913) Die Kinetik der Invertinwirkung. *Biochem. Z. 49*, 333−369.

(29) Engel, P. (1996) *Enzymology Labfax*, 1st ed., pp 200−210, Academic Press, San Diego.

(30) Dowd, J. E., and Riggs, D. S. (1965) A Comparison of Estimates of Michaelis-Menten Kinetic Constants from Various Linear Transformations. *J. Biol. Chem. 240*, 863−869.

(31) Eadie, G. S. (1942) The inhibition of cholinesterase by physostigmine and prostigmine. *J. Biol. Chem. 146*, 85−93.

(32) Hofstee, B. H. (1959) Non-inverted versus inverted plots in enzyme kinetics. *Nature 184*, 1296−1298.

(33) Wells, T. N., and Fersht, A. R. (1986) Use of binding energy in catalysis analyzed by mutagenesis of the tyrosyl-tRNA synthetase. *Biochemistry 25*, 1881−1886.

(34) Jordanova, A., Thomas, F. P., Guergueltcheva, V., Tournev, I., Gondim, F. A., Ishpekova, B., De Vriendt, E., Jacobs, A., Litvinenko, I., Ivanova, N., Buzhov, B., De Jonghe, P., Kremensky, I., and Timmerman, V. (2003) Dominant intermediate Charcot-Marie-Tooth type C maps to chromosome 1p34-p35. *Am. J. Hum. Genet. 73*, 1423−1430.

(35) Jia, J., Li, B., Jin, Y., and Wang, D. (2003) Expression, purification, and characterization of human tyrosyl-tRNA synthetase. *Protein Expression Purif. 27*, 104−108.

(36) Rossi, A., Paradiso, C., Cioni, R., Rizzuto, N., and Guazzi, G. (1985) Charcot-Marie-Tooth disease: study of a large kinship with an intermediate form. *J. Neurol. 232*, 91−98.

(37) Villanova, M., Timmerman, V., De Jonghe, P., Malandrini, A., Rizzuto, N., Van Broeckhoven, C., Guazzi, G., and Rossi, A. (1998) Charcot-Marie-Tooth disease: an intermediate form. *Neuromuscul. Disord. 8*, 392−393.

(38) Storkebaum, E., Leitao-Goncalves, R., Godenschwege, T., Nangle, L., Mejia, M., Bosmans, I., Ooms, T., Jacobs, A., Van Dijck, P., Yang, X. L., Schimmel, P., Norga, K., Timmerman, V., Callaerts, P., and Jordanova, A. (2009) Dominant mutations in the tyrosyl-tRNA synthetase gene recapitulate in Drosophila features of human Charcot-Marie-Tooth neuropathy. *Proc. Natl. Acad. Sci. U.S.A. 106*, 11782−11787.

(39) Wakasugi, K., and Schimmel, P. (1999) Two distinct cytokines released from a human aminoacyl-tRNA synthetase. *Science (New York, N.Y.) 284*, 147−151.

(40) Guo, M., Schimmel, P., and Yang, X. L. (2010) Functional expansion of human tRNA synthetases achieved by structural inventions. *FEBS Lett. 584*, 434−442.

(41) Kawamata, H., Magrane, J., Kunst, C., King, M. P., and Manfredi, G. (2008) Lysyl-tRNA synthetase is a target for mutant SOD1 toxicity in mitochondria. *J. Biol. Chem. 283*, 28321−28328.

(42) Nangle, L. A., Zhang, W., Xie, W., Yang, X. L., and Schimmel, P. (2007) Charcot-Marie-Tooth disease-associated mutant tRNA synthetases linked to altered dimer interface and neurite distribution defect. *Proc. Natl. Acad. Sci. U. S. A. 104*, 11239−11244.

(43) Aguzzi, A., O'Connor, T. Protein aggregation diseases: pathogenicity and therapeutic perspectives, *Nat. Rev. Drug Discovery 9*, 237−248.

(44) Lee, J. W., Beebe, K., Nangle, L. A., Jang, J., Longo-Guess, C. M., Cook, S. A., Davisson, M. T., Sundberg, J. P., Schimmel, P., and Ackerman, S. L. (2006) Editing-defective tRNA synthetase causes protein misfolding and neurodegeneration. *Nature 443*, 50−55.

(45) Fechter, P., Rudinger-Thirion, J., Theobald-Dietrich, A., and Giege, R. (2000) Identity of tRNA for yeast tyrosyl-tRNA synthetase: tyrosylation is more sensitive to identity nucleotides than to structural features. *Biochemistry 39*, 1725−1733.

(46) Zhang, C. M., Perona, J. J., Ryu, K., Francklyn, C., and Hou, Y. M. (2006) Distinct kinetic mechanisms of the two classes of Aminoacyl-tRNA synthetases. *J. Mol. Biol. 361*, 300−311.

(47) Gruic-Sovulj, I., Rokov-Plavec, J., and Weygand-Durasevic, I. (2007) Hydrolysis of non-cognate aminoacyl-adenylates by a class II aminoacyl-tRNA synthetase lacking an editing domain. *FEBS Lett. 581*, 5110−5114.

(48) Yang, X. L., Skene, R. J., McRee, D. E., and Schimmel, P. (2002) Crystal structure of a human aminoacyl-tRNA synthetase cytokine. *Proc. Natl. Acad. Sci. U.S.A. 99*, 15369−15374.

(49) Iwata, A., Christianson, J. C., Bucci, M., Ellerby, L. M., Nukina, N., Forno, L. S., and Kopito, R. R. (2005) Increased susceptibility of cytoplasmic over nuclear polyglutamine aggregates to autophagic degradation. *Proc. Natl. Acad. Sci. U.S.A. 102*, 13135−13140.

(50) Tsunoda, M., Kusakabe, Y., Tanaka, N., Ohno, S., Nakamura, M., Senda, T., Moriguchi, T., Asai, N., Sekine, M., Yokogawa, T., Nishikawa, K., and Nakamura, K. T. (2007) Structural basis for recognition of cognate tRNA by tyrosyl-tRNA synthetase from three kingdoms. *Nucleic Acids Res. 35*, 4289−4300.

(51) Tsunoda, M., Kusakabe, Y., Tanaka, N., Ohno, S., Nakamura, M., Senda, T., Sekine, M., Yokogawa, T., Nishikawa, K., and Nakamura, K. T. (2004) Three-dimensional structure of the ternary complex of yeast tyrosyl-tRNA synthetase. *Nucleic Acids Symp. Ser. (Oxford)*, 155−156.

(52) Collaborative Computational Project, N. (1994) The CCP4 suite: programs for protein crystallography. *Acta Crystallogr. 50*, 760−763.

(53) Krissinel, E., and Henrick, K. (2004) Secondary-structure matching (SSM), a new tool for fast protein structure alignment in three dimensions. *Acta Crystallogr. 60*, 2256−2268.

(54) The PyMOL Molecular Graphics System, version 1.3, Schrodinger, LLC.

(55) Fersht, A.R., Knill-Jones, J. W., Bedouelle, H., and Winter, G. (1988) Reconstruction by site-directed mutagenesis of the transition state for the activation of tyrosine by the tyrosyl-tRNA synthetase: a mobile loop envelopes the transition state in an induced-fit mechanism. *Biochemistry 27*, 1581−1587.

(56) Korneliuk, A. I., Kurochkin, I. V., and Matsuka, G. (1988) [Tyrosyl-tRNA synthetase from the bovine liver. Isolation and physico-chemical properties]. *Mol. Biol. (Kiev) 22*, 176−186.

(57) Deak, F., and Denes, G. (1978) Purification and some properties of rat liver tyrosyl-tRNA synthetase. *Biochim. Biophys. Acta 526*, 626−634.

(58) Warner, C. K., and Jacobson, K. B. (1976) Mechanisms of suppression in Drosophila. IV. Specificity and properties of tyrosyl-tRNA synthetase. *Can. J. Biochem. 54*, 650−656.

(59) Kucan, Z., and Chambers, R. W. (1973) Purification of tyrosine: tRNA ligase from Saccharomyces cerevisiae alphaS288C. *J. Biochem. 73*, 811−819.

(60) Quivy, J. P., and Chroboczek, J. (1988) Tyrosyl-tRNA synthetase from wheat germ. *J. Biol. Chem. 263*, 15277−15281.